sel-7, a Positive Regulator of *lin-12* Activity, Encodes a Novel Nuclear Protein in *Caenorhabditis elegans*

Jiabin Chen,* Xiajun Li[†,1] and Iva Greenwald*[,‡,2]

**Department of Biochemistry and Molecular Biophysics,* [†]*Integrated Program in Cellular, Molecular and Biophysical Studies and* [‡]*Howard Hughes Medical Institute, Columbia University, College of Physicians and Surgeons, New York, New York 10032*

Manuscript received September 2, 2003
Accepted for publication October 1, 2003

ABSTRACT

Suppressor genetics in *C. elegans* has identified key components of the LIN-12/Notch signaling pathway. Here, we describe a genetic and molecular characterization of the suppressor gene *sel-7*. We show that reducing or eliminating *sel-7* activity suppresses the effects of constitutive *lin-12* activity, enhances the effects of partially reduced *lin-12* activity, and causes a synthetic Lin-12(0) phenotype when combined with a null mutation in the *sel-12* presenilin gene. These observations suggest that *sel-7* is a positive regulator of *lin-12* activity. We also show that SEL-7 encodes a novel nuclear protein. Through yeast two-hybrid screening, we identified an apparent interaction partner, K08E3.8, that also interacts with SEL-8, a known component of the nuclear complex that forms upon LIN-12 activation. Our data suggest potential roles for SEL-7 in the assembly or function of this nuclear complex.

CELLS with equivalent potentials are specified via cell-cell interactions to adopt distinct fates during animal development. Many interactions are mediated by the receptor LIN-12/Notch (Greenwald 1998). LIN-12/Notch is activated by binding of a ligand of the DSL (*D*elta/*S*errate/*L*AG-2) family. Ligand binding induces at least two proteolytic cleavages, one in the extracellular domain of the receptor and the other in the transmembrane domain. The latter cleavage releases the intracellular domain of the receptor, which translocates into the nucleus and forms a transcriptional activation complex with LAG-1 (known as Suppressor of Hairless in Drosophila and CBF1 or RBP-J in mammals) and other cofactors (Weinmaster 2000).

The anchor cell (AC)/ventral uterine precourser cell (VU) decision is a well-characterized cell fate decision that is mediated by LIN-12 in *Caenorhabditis elegans* (Greenwald 1998). In wild-type hermaphrodites, two gonadal cells interact with each other so that one becomes the AC and the other becomes the VU. Missense mutations or truncations that cause constitutive *lin-12* activity cause both cells to become VUs, so that an AC is missing; the absence of an AC results in an egg-laying defective (Egl) phenotype that is easily visualized in the dissecting microscope. Extragenic suppressors defined by reversion of the 0 AC-Egl defect have identified a number of *sel* (**s**uppressor/**e**nhancer of *lin-12*) genes (Tax *et al.* 1997; L. Vallier, I. Katic, J. Chen and I. Greenwald, unpublished data). Characterized *sel* genes have been found to encode components important for LIN-12/Notch activity. Among these are two membrane-associated proteases that mediate proteolytic cleavage of LIN-12/Notch after ligand binding: SEL-12, an ortholog of human presenilin, which mediates transmembrane cleavage of LIN-12/Notch (Levitan and Greenwald 1995; De Strooper *et al.* 1999; Struhl and Greenwald 1999), and SUP-17, an ortholog of Drosophila Kuzbanian and a mammalian ADAM protein, which is likely to mediate cleavage of the extracellular domain (Wen *et al.* 1997). Another *sel* gene, *sel-5*, encodes a cytoplasmic serine/threonine kinase that may influence LIN-12 trafficking (Fares and Greenwald 1999).

In contrast to the SEL proteins that appear to have enzymatic activities, SEL-8 is a novel, glutamine-rich nuclear protein (Doyle *et al.* 2000; Petcherski and Kimble 2000a). SEL-8 is required for LIN-12/Notch activity in *C. elegans* and appears to form a bridge between LAG-1 and the intracellular domain of LIN-12 (Doyle *et al.* 2000; Petcherski and Kimble 2000a). There is no primary sequence homology with non-nematode proteins; however, SEL-8 has been proposed to serve as the counterpart to the glutamine-rich protein Mastermind of Drosophila and mammals (Petcherski and Kimble 2000b). Mastermind has been shown to be a component of the transcriptional activation complex that contains Suppressor of Hairless and the Notch intracellular domain (Wu *et al.* 2000; Kitagawa *et al.* 2001).

Here we report the characterization of another *sel* gene, *sel-7* (first identified in Tax *et al.* 1997), which,

[1]*Present address:* Department of Genetics, Harvard Medical School, Boston, MA 02115.

[2]*Corresponding author:* Department of Biochemistry and Molecular Biophysics, 701 W. 168th St., Room 720, College of Physicians and Surgeons, Columbia University, New York, NY 10032.
E-mail: greenwald@cancercenter.columbia.edu

like *sel-8*, also encodes a novel nuclear protein. Our analysis is consistent with a role for SEL-7 in the formation or function of the nuclear complex that activates expression of LIN-12/Notch target genes.

MATERIALS AND METHODS

General *C. elegans* methods and strains: Standard methods as described in Brenner (1974) were used for handling, maintenance, and genetic analysis of *C. elegans*. Experiments were performed at 20° unless otherwise indicated. The wild-type parent for all strains was *C. elegans* var. Bristol N2 (Brenner 1974), except for mapping experiments done with the Hawaiian strain CB4856. The main alleles used in this work are LG I: *smg-1(r861), unc-54(r293)* (Hodgkin *et al.* 1989); LG III: *lin-12(n302, n137, n950)* (Greenwald *et al.* 1983), *lin-12(ar170)* (Hubbard *et al.* 1996), *glp-1(ar202)* (Pepper *et al.* 2003), *glp-1 (e2141, e2142)* (Priess *et al.* 1987); and LG X: *sel-7 (n1253, ar516, ar523, ar586)* (Tax *et al.* 1997 and this study), *sel-12 (ar171)* (Levitan and Greenwald 1995).

Transgenes: *arIs12[lin-12(intra)]* expresses the intracellular domain of LIN-12 under the control of *lin-12* regulatory sequences and is marked with the dominant marker *rol-6 (su1006)* (Struhl *et al.* 1993). *arIs37* expresses a secreted form of green fluorescent protein (GFP) under the control of a muscle-specific promoter, so that GFP is secreted into the pseudocoelom; uptake of GFP from the pseudocoelom can be used to help visualize coelomocytes (Fares and Greenwald 2001). *arIs51 [cdh-3::gfp]* (Karp and Greenwald 2003) expresses GFP under the control of *cdh-3* regulatory sequences and can be used to help visualize anchor cells (Pettitt *et al.* 1996).

Additional information about the alleles listed above and about *unc-1(e538), unc-3(e151), unc-84(e1410)*, and other markers used for mapping and for facilitating genetic analyses in this work can be found via Wormbase at http://www.wormbase.org.

Mutant analysis and scoring: Strains were grown and scored at 20° unless otherwise specified. Phenotypes were assessed as follows. For egg-laying defect, L4 larvae were picked onto individual plates and scored 2 or 3 days later. An animal was scored as Egl^+ if it laid eggs and as Egl if it did not lay eggs or formed a bag of larvae during this period of time. The egg-laying ability of sterile individuals could not be assessed. For ACs, strains generally contained *arIs51*, which expresses GFP in the AC. L3 larvae were scored using Nomarski optics, and ACs were identified by both morphology and GFP expression. For multivulva, L4 larvae were picked onto individual plates and checked for the number of pseudovulvae the next day. Egg-laying-competent hermaphrodites were excluded from the final tallies, since the presence of an AC causes a normal vulva to form. For coelomocytes, the number of coelomocytes was determined in L4 larvae or young adults both by their characteristic morphology under Nomarski optics and by accumulation of GFP. For germline proliferation, individual *glp-1 (ar202)* L4 larvae grown at 20° were transferred to the nonpermissive temperature, 25°, and scored for progeny production. For embryonic lethality, individual *glp-1(e2142)* L4 larvae were transferred to fresh plates every day for 3 consecutive days, and the eggs laid on the plates were scored for hatching. This assay was conducted at 15°.

In addition to canonical *lin-12* phenotypes, we also observed that the double mutant *sel-7(n1253) unc-3(e151)* formed dauers at 80% penetrance (25/30) at 25°, whereas neither single mutant did (data not shown). Loss of *lin-12* activity caused by alleles such as *lin-12(oz48)* has been observed to enhance the frequency of dauer formation in dauer-constitutive mutant backgrounds (Levitan and Greenwald 1998). To assess whether the synthetic dauer-constitutive phenotype resulted from reduced *lin-12* activity in a *sel-7* mutant, we examined *lin-12(oz48); unc-3(e151)* and found that it does not show a daf-c phenotype (0/51). In addition, it has been observed that *unc-3* becomes dauer constitutive at 27° (Ailion and Thomas 2000). We therefore tested whether *sel-7* forms dauers at 27°, but found that it does not. We did not attempt to determine the basis for the synergy between *sel-7* and *unc-3*.

Genetic mapping of *sel-7* locus and sequencing: *sel-7* has been previously mapped between *unc-84* and *unc-3* on LG X (Tax *et al.* 1997). We used single-nucleotide polymorphisms (SNPs) on LG X to refine the map position of *sel-7(n1253)*. We identified the following SNPs: xl1 on cosmid F16B12; xl2F1R1 on K04C1; xl3DoaF4R7 on C11H1; xl4F7R7A and xl5F7R7B on T14C1; and xl6F2R2 on M163; xl7F2R2, jlF3R3, and jcF4R4 on K04G11. Males of the Hawaiian strain CB4856 were crossed to *unc-84 sel-7(n1253) unc-3* hermaphrodites, and F_1 heterozygotes segregated Unc-84 non-Unc-3 F_2 recombinants. The presence of *sel-7(n1253)* in the recombinants was assessed later by the ability to suppress *lin-12(n302)*. A total of 101 recombinants were obtained and analyses of the SNPs in these recombinants enabled us to map *sel-7* between jlF3R3 and jcF4R4 on K04G11. We then sequenced the predicted genes on this cosmid. PCR product using one pair of primers, K04G11.2F1: 5′-TCTCTCGGATGGTACATATCGG-3′ and K04 G11.2R1: 5′-TACTTCAAACGTAAGGGGTG-3′ contains a C-to-T mutation in the predicted gene K04G11.2.

cDNA cloning and correction of the GENEFINDER prediction for K04G11.2: To determine the gene structure of *sel-7* in the absence of any available expressed sequence tags, we screened three cDNA libraries and subsequently used the ProQuest cDNA library (GIBCO BRL, Gaithersburg, MD, catalog no. 10835) to amplify pieces of *sel-7* cDNA. Two overlapping fragments were amplified by using primer sets (1) 5pPC86 (5′-TATAACGCGTTTGGAATCACT-3′, recommended by the manufacturer) and K2C2 (5′-CTCGGTTTCCTTCGGCGA TTG-3′) and (2) K2C.33 (5′-CGAGGATTCTGATGGCGACT TAG-3′) and 3pPC86 (5′-GTAAATTTCTGGCAAGGTAGAC-3′, recommended by the manufacturer). The two pieces were then pasted together by PCR. Sequencing of the cDNA thus obtained revealed that the predicted gene K04G11.2 does not contain the entire coding region of *sel-7*. The first four exons of *sel-7* correspond to K04G11.2 (rapid amplification of cDNA ends experiments showed that *sel-7* was transpliced to a nonclassic spliced leader, 5′-GGTTTAATTACCCAAGTTTGAG-3′) and then a 5-kb intergenic region was spliced out between the fourth and the fifth exon. The last three exons (fifth, sixth, and seventh) encompass what had been predicted as K04G11.6. This gene structure was further confirmed by RNA-mediated interference (RNAi) and the identification of a mutation in the fifth exon in another *sel-7* allele, *ar516*.

RNAi: *For dsRNA micro-injection:* Double-stranded RNA (dsRNA) was synthesized *in vitro* using the cloned PCR fragment amplified from N2 genomic DNA as template. To confirm the cloning and the gene structure of *sel-7*, the following pairs of primers were used to amplify different regions of *sel-7* genomic sequences: (1) K04G11.2F1 (5′-TCTCTCGGATGG TACATATCGG-3′) and K2R3 (5′-CGTGTTGTCTGCTTTC AATCG-3′), (2) 905R1(5′-GGTTTAAGAATTCCCGCACCG-3′) and VKF0 (5′-TGAAGAGATAATGCTAGGCGAG-3′), (3) 905 R1 and VKF1 (5′-CTAGATCAACGTTCACTGGTGG-3′), and (4) K2C.36 (5′-AGCCAGCTGAGTAAAGC-3′) and VKF0. Both T7 and T3 polymerases were added to the same *in vitro* transcription reaction, or each strand of RNA was synthesized with T7 or T3 polymerase alone. The RNA was purified on RNeasy columns (QIAGEN, Valencia, CA) and then allowed to anneal

in 0.5× injection buffer (Mello and Fire 1995). dsRNA was micro-injected into the pseudocoelomic space of young adult hermaphrodites. Injected worms were individually placed and their F_1 progeny were scored. For RNA feeding, full cDNA of *sel-7* (see above) and the cDNA clones of F13B10.1B and K08E3.8 pulled out from the yeast two-hybrid screens (see below) were cloned into vector pPD129.36 (Timmons *et al.* 2001) and then transformed into bacterial strain HT115 (Timmons and Fire 1998; Timmons *et al.* 2001). Eggs or arrested L1 larvae were placed onto a lawn of such bacteria and relevant phenotypes were later scored.

Plasmid construction: *sel-7 cDNA clone: sel-7* cDNA was obtained as described above. A *Sal*I site was generated before the stop codon by PCR with a pair of complementary primers (5′-GACCCAAGTCTATTCAAGGTTGTCGACTAAAATCCT CGCCTAGC-3′; the underlined sequence indicates the *Sal*I site). GFP was excised from a KSGFPS65T vector (pPD114.38; A. Fire, personal communication) with *Sal*I and inserted in frame into the cDNA construct. The 5′ untranslated region of *sel-12* was excised with *Sac*I and *Not*I from the vector superPin2 (a modified version of Pin2; see Fares and Greenwald 1999, which has additional cloning sites), which contains the whole genomic region of *sel-12*, and then inserted before the *sel-7* cDNA::gfp construct. For yeast two-hybrid plasmids, vectors were provided by ProQuest. pPC86 contains the GAL4 activation domain, and pDBLeu contains the GAL4 DNA-binding domain. Full-length cDNAs of *lag-1*, *lin-12(intra)*, *sel-7*, *sel-8*, and *skip* (Zhou *et al.* 2000) were cloned either between *Sal*I and *Not*I sites or between *Sal*I and *Spe*I sites on both plasmids except for the following constructs. Full-length cDNA of *lag-1* was used for pPC86, but a truncated form that runs from Met630 of LAG-1 until the end of the protein was used for insertion into pDBLeu. Two forms of LIN-12(intra) were used; both start at Pro930, but end differently. For pPC86, LIN-12(intra) ends at the end of the protein. For pDBLeu, the insertion ends at Val1320 and a stop codon was inserted after the valine. For yeast three-hybrid plasmids, the third, non-GAL4-domain-containing yeast expression vector pRST was generated on the basis of pRS416. The promoter P_{ADH} and the terminator T_{ADH} were excised from pPC86 with *Kpn*I, *Hin*dIII, and *Sma*I, *Bam*HI, respectively, and inserted into pRS416 between the corresponding sites. Full-length cDNAs of *lag-1*, *lin-12(intra)* (Pro930 till TAA), and K08E3.8 were then cloned into the pRST vector.

Yeast two-hybrid and three-hybrid assays: Plasmids, yeast cells, and protocols for the yeast two-hybrid and three-hybrid assays were provided by the ProQuest two-hybrid system (GIBCO BRL, catalog no. 10835). The yeast strain used for all the experiments in this study was MaV203, and all yeast cells were cultured at 30°. For yeast transformation, cells were streaked out from frozen stock and four single colonies were picked and suspended in YPAD medium and inoculated at 30° for overnight. On the next morning, the cells were diluted to OD_{600} = 0.1 and cultured until OD_{600} reached 0.4. Cells were collected by centrifuge and transformed with desired DNA according to the protocol provided by the manufacturer. Cells were then spread on proper nutrient-deficient plates (SC-Leu-Trp for two-hybrid assays and SC-Leu-Trp-Ura for three-hybrid assays) for plasmid selection and incubated at 30° for 72 hr. For interaction detection, four colonies from each plate were patched onto a new plate, allowed to grow for 18 hr, and then replica plated onto an 82-mm nitrocellulose membrane. Cells were left on the membrane on top of YPAD medium for another 24 hr at 30°, and the interaction was then tested by β-galactosidase assay described as follows. The membrane was lifted off the plate, frozen at −80° for 20–30 min, transferred onto two layers of filter paper preabsorbed in the reaction buffer (5 ml Z-buffer, 30 μl β-mercaptoethanol, 300 μl 3% X-Gal for each membrane), and then incubated at 37° for the reaction to take place. The appearance of blue colony color was assessed every hour for 1–4 hr and then again after overnight incubation.

Yeast two-hybrid screen: The ProQuest two-hybrid *C. elegans* cDNA library was amplified according to the protocol provided by the manufacturer. pDBLeu-*sel-7*cDNA (see the plasmid construction above) was first transformed into yeast strain MaV203, and a single colony was picked and cultured in 2 ml SC-Leu medium at 30° overnight. On the next day, the cells were diluted into 50 ml SC-Leu medium and cultured again at 30° overnight. On the third morning, cells were diluted into 300 ml SC-Leu medium so that the OD_{600} was ~0.1 and then cultured at 30° until OD_{600} reached 0.5. Cells were collected and transformed with 25 μl cDNA library DNA (750 μg/ml) and spread on 15-cm SC-Leu-Trp plates. Plates were incubated at 30° for 72 hr, and colonies were replica plated onto 13.52-cm nitrocellulose membrane filters. Positive colonies were selected by β-galactosidase assay as follows: Membranes were frozen at −80° for 30 min, transferred onto two layers of filter paper preabsorbed in the reaction buffer (15 ml Z-buffer, 39 μl β-mercaptoethanol, 300 μl 3% X-Gal for each membrane) and then incubated at 30° overnight. Blue colonies were then picked and streaked onto SC-Leu-Trp plates. Single colonies were picked and DNA was extracted with DNA-Pure plasmid mini-prep kit (CPG) and sequenced for its identity. We did two independent screens, and 15 blue colonies were obtained. Of these 15, 12 regrew on SC-Leu-Trp plates; these 12 colonies represented three different genes. We then tested their self-activation by transforming them with an empty pDBLeu plasmid using the methods described above. One of the three genes turned out to be self-activating and was removed from the positive list. Therefore, we obtained two different *sel-7* interacting genes, F13B10.1B and K08E3.8, described further in the text.

RESULTS

***sel-7* is a positive regulator of *lin-12* activity in the AC/VU decision:** In wild-type hermaphrodites, two initially equivalent cells, Z1.ppp and Z4.aaa, interact with each other so that one becomes the AC and the other becomes the VU; each cell has an equal chance to become the AC. In *lin-12(d)* mutants such as *lin-12(n302)*, LIN-12 is constitutively active (Greenwald and Seydoux 1990), both Z1.ppp and Z4.aaa become VUs, and the worm has no AC and hence is vulvaless and egg-laying defective (0 AC-Egl). *sel-7(n1253)* was originally identified by Tax *et al.* (1997) as a suppressor of the 0 AC-Egl defect of *lin-12(n302)*, and we identified additional alleles of *sel-7* in a similar screen (L. Vallier, I. Katic, J. Chen and I. Greenwald, unpublished observations). We have used *sel-7(n1253)* for most genetic experiments; sequence analysis described below suggests that it is likely to be a strong loss-of-function or null allele.

We did not observe any overt phenotype of *sel-7* in an otherwise wild-type background, which is consistent with the observation by Tax *et al.* (1997). However, genetic interactions with different classes of *lin-12* alleles suggest that *sel-7* is a positive regulator of *lin-12* activity (Tables 1 and 2). First, *sel-7(n1253)* suppresses the 0 AC-Egl phenotype caused by constitutively active LIN-12.

TABLE 1

***sel-7* reduces the activity of different constitutively active forms of LIN-12**

Relevant genotype	0 AC-Egl/total (%)
N2	Many (0)
lin-12(n302, n137, n950)	Many (100)
lin-12(n302); sel-7(n1253)	145/263 (55)[a]
lin-12(n302); sel-7(ar523)	130/236 (55)
lin-12(n950); sel-7(n1253)	41/51 (80)
lin-12(n137); sel-7(n1253)	49/50 (98)
arIs12 [lin-12(intra)][b]	30/46 (65)
arIs12[lin-12(intra)]; sel-7(n1253)][b]	15/64 (23)

[a] Tax *et al.* (1997) reported 47% for this genotype.
[b] Also contains *unc-3(e151)* and *arIs51[cdh-3::gfp]*. These two strains were grown and scored in parallel at 15°.

TABLE 2

***sel-7* enhances a *lin-12* hypomorphic allele and synergizes with a *sel-12* null allele**

Relevant genotype	2AC/total (%)
lin-12(ar170)[a]	24/49 (50)
lin-12(ar170); sel-7(n1253)[a]	25/25 (100)
sel-7(n1253)[a]	0/44 (0)
sel-12(ar171)[b]	0/33 (0)
sel-12(ar171) sel- 7(n1253)[b]	6/80 (7.5)

[a] Also contains *unc-3(e151)* and *arIs51[cdh-3::gfp]*.
[b] Also contains *unc-1(e528)* and *arIs51[cdh-3::gfp]*.

For *lin-12(d)* missense mutations, which can be arranged into an allelic series (Greenwald *et al.* 1983), the degree of suppression roughly correlates with the strength of the *lin-12(d)* allele: *sel-7(n1253)* is a more efficient suppressor of *lin-12(n302)*, which has a relatively lower level of constitutive *lin-12* activity, than of *lin-12(n137)*, which is relatively "stronger." Second, *sel-7* enhances the 2AC defect of *lin-12(ar170)*, a partial loss-of-function allele.

In addition, loss of *sel-7* activity displays synergy with loss of *sel-12* activity (Table 2). *sel-12* is another positive regulator of the LIN-12/Notch signal transduction pathway. *sel-12* encodes a homolog of human presenilin and mediates the transmembrane cleavage that releases the LIN-12 intracellular domain from its membrane tether. Neither *sel-12* nor *sel-7* alone displays any defect in the AC/VU decision, yet the *sel-12 sel-7* double mutant displays an incompletely penetrant 2AC phenotype, reminiscent of *lin-12* partial loss-of-function alleles (Table 2). This result suggests that *lin-12* activity is lower in a *sel-7* mutant background, although not low enough to cause defects in the AC/VU decision.

Loss of *sel-7* activity also suppresses the 0 AC phenotype caused by *lin-12(intra)*, which, like *lin-12(d)* mutations, causes constitutive LIN-12 activity. LIN-12(intra) resembles the cleavage product produced after LIN-12 activation, so the ability of *sel-7* to suppress *lin-12(intra)* is consistent with a role for *sel-7* downstream of the activated receptor (Table 1).

***sel-7* activity in other *lin-12*- or *glp-1*-mediated cell fate decisions:** We examined the ability of *sel-7* to suppress *lin-12(d)* mutations for defects in the two cell fate decisions that have served as the basis for other genetic studies of *lin-12*, vulval precursor cell (VPC) specification and the decision made by certain mesodermal cells between the coelomocyte (cc) and sex myoblast fate. We also examined the ability of *sel-7* to suppress or enhance *glp-1* alleles for defects in germline proliferation and embryonic development.

VPC specification: There are six VPCs, consecutively numbered P3.p–P8.p. LIN-12/Notch signaling, along with other signaling events, specifies their fates (reviewed in Greenwald 1998). In a wild-type hermaphrodite, only P5.p and P7.p adopt a fate called "2°." However, in a strong *lin-12(d)* background, such as *lin-12(n137)* and *lin-12(n950)*, all six VPCs adopt the 2° fate, resulting in a distinctive Multivulva (Muv) phenotype. *sel-7* does not suppress the Muv phenotype caused by *lin-12(d)* mutations, suggesting that *sel-7* does not function in the VPCs or that loss of *sel-7* activity does not reduce *lin-12* activity sufficiently to suppress the Muv phenotype; alternatively, there may be functional redundancy between SEL-7 and another, unknown, protein (Table 3).

Sex mesoblast/coelomocyte specification: Two cells, M.drpa and M.dlpa, give rise postembryonically to coelomocytes that are located dorsally and generally posterior to the gonad. In *lin-12(d)* mutants, M.drpa and M.dlpa are transformed into their ventral equivalents and instead become sex mesoblasts. *sel-7* partially suppresses this transformation (Table 3).

glp-1-mediated decisions: Tax *et al.* (1997) reported that *sel-7(n1253)* enhanced the effects of the *glp-1(e2141)* loss-of-function allele for embryonic lethality and brood size, suggesting that *sel-7* plays a role in cell fate decisions mediated by *glp-1*. However, we did not see significant interaction of *sel-7(n1253)* with other *glp*-1 alleles. *sel-7* did not enhance the embryonic lethality of *glp-1(e2142)* (Priess *et al.* 1987): 30% (38/125) of *glp-1(e2142)* embryos arrested at 15°, similar to 21% (25/120) of *glp-1 (e2142); sel-7(n1253)* and 32% (55/172) of *glp-1(e2142); sel-7(ar516)* embryos. *sel-7* did not suppress the sterility caused by the constitutively active allele *glp-1(ar202)* (Pepper *et al.* 2003): 96% (54/56) of *glp-1(ar202)* hermaphrodites were sterile at 25°, as were 91% (52/57) of *glp-1(ar202); sel-7(n1253)* hermaphrodites.

Molecular identification of *sel-7:* *sel-7* had been previously mapped between *unc-84* and *unc-3* on LG X (Tax *et al.* 1997). We identified new SNPs (see materials and methods) and mapped *sel-7* onto one cosmid, K04G11 (Figure 1A). We began sequencing DNA prepared from *sel-7(n1253)* worms for predicted genes on this cosmid and found a point mutation in a predicted gene called

TABLE 3

***sel-7* affects a subset of *lin-12/Notch*-mediated cell fate decisions**

Genotype	Muv/*n* (%)	Average no. of pseudovulvae	Transformed cc/*n* (%)[b,c]
lin-12(n137)	52/52 (100)	4.8	16/36 (44.5)
lin-12(n137); sel-7(n1253)	105/105 (100)	4.7[a]	9/41 (22)
lin-12(n950)	56/56 (100)	4.8	ND
lin-12(n950); sel-7(n1253)	79/79 (100)	4.8[a]	ND

For each set of genotypes, strains were grown and scored in parallel. ND, not determined.

[a] Average number of pseudovulvae calculated from 55 hermaphrodites for *lin-12(n137); sel-7* and from 37 hermaphrodites for *lin-12(n950); sel-7*.

[b] A GFP marker, *arIs37* (see MATERIALS AND METHODS), was used to help score the coelomocytes.

[c] Percentage of hermaphrodites that have no postembryonic coelomocytes. In wild-type hermaphrodites, a few (4/45) exhibit only one coelomocyte using this scoring criterion, while all others (41/45) have two coelomocytes.

K04G11.2, suggesting that that this gene corresponded to *sel-7*.

Our analysis of cDNAs (see MATERIALS AND METHODS), however, revealed that K04G11.2 was actually joined to another predicted gene that lay in the same orientation, then called "K04G11.6." Within the 5-kb interval separating K04G11.2 and K04G11.6 was another predicted gene in the opposite orientation. The composite gene, now listed as K04G11.2 in Wormbase, contains seven exons; the first four were originally from K04G11.2. Corroborating evidence for this structure is described in the next section.

Corroborating evidence that K04G11.2 is *sel-7* and the *sel-7* null phenotype: We have verified that the composite K04G11.2/K04G11.6 (now listed as K04G11.2) corresponds to *sel-7* by three criteria. The first two of these criteria also indicate that the null phenotype of *sel-7* is Sel; *i.e.*, K04G11.2 acts as a suppressor/enhancer of *lin-12* and does not cause a phenotype that is readily detected in an otherwise wild-type background.

First, we found sequence alterations associated with other *sel-7* alleles throughout the composite gene (Figure 1B). The sequence analysis also suggests that most or all of the *sel-7* alleles that we obtained are strong loss-of-function or null mutations. *sel-7(n1253)*, the reference allele used for most of our genetic analysis, is predicted to truncate the SEL-7 protein about halfway through, at amino acid 171; although it seems likely, we cannot conclude from the sequence information that *sel-7(n1253)* is a molecular null. *sel-7(ar523)* appears likely to be a molecular null allele. *sel-7(ar523)* is predicted to truncate SEL-7 at amino acid 55 and behaves like *sel-7(n1253)* in terms of suppression of *lin-12(n302)* (Table 1). *sel-7(n1253)* does not have any visible phenotype or any effect on the number of ACs in an otherwise wild-type background.

Second, we injected four different dsRNAs, corresponding to different regions of the composite gene, into *lin-12(n302)* hermaphrodites and assayed the progeny of injected hermaphrodites for egg-laying ability (see Figure 1A). All four dsRNAs suppressed the 0 AC-Egl phenotype of *lin-12(n302)*: For a dsRNA corresponding to exons 1–4, 22/29 injected hermaphrodites gave egg-laying progeny; for exons 5 and 6, 2/2; for exons 6 and 7, 5/5; and for exons 5–7, 8/9. The fact that depletion of *sel-7* activity by RNAi suppresses *lin-12(n302)* corroborates the inference from sequence analysis that *sel-7* mutations reduce or eliminate *sel-7* activity.

Third, we obtained evidence that a cDNA corresponding to the corrected K04G11.2 sequence can complement *sel-7(n1253)*. We were unable to achieve good expression or rescue with a genomic fragment corresponding to the *sel-7* region in simple arrays (data not shown), a problem also encountered in the analysis of *sel-5* (FARES and GREENWALD 1999) and other genes (J. HSIEH, S. KOSTAS and A. FIRE, personal communication). We therefore expressed a composite *K04G11.2::gfp* cDNA under the control of *sel-12* regulatory sequences in a complex array. As shown in Table 1, *lin-12(ar170); sel-7(n1253)* hermaphrodites display a completely penetrant 2AC phenotype. We crossed *arEx434*, an extrachromosomal array that gives detectable expression of GFP-tagged SEL-7, into the *lin-12(ar170); sel-7(n1253)* background and observed that 50/96 hermaphrodites had 1AC. This observation supports the identification of K04G11.2 as *sel-7* and suggests furthermore that the SEL-7::GFP protein is functional.

SEL-7 is a nuclear protein: We analyzed the predicted SEL-7 protein using two programs, SMART (http://smart.embl-heidelberg.de/) and PESTFIND (http://bioweb.pasteur.fr/seqanal/interfaces/pestfind-simple.html) and found that SEL-7 contains two predicted PEST sequences, but no other distinctive amino acid sequence motifs (Figure 1B). BLAST searches identified highly similar sequences in *Caenorhabditis briggsae* and in three parasitic nematode species, *Brugia malayi*, *Oncocerca volvulus*, and *Ancylostoma ceylanicum* (Figure 1C), but did not identify similar sequences in other organisms.

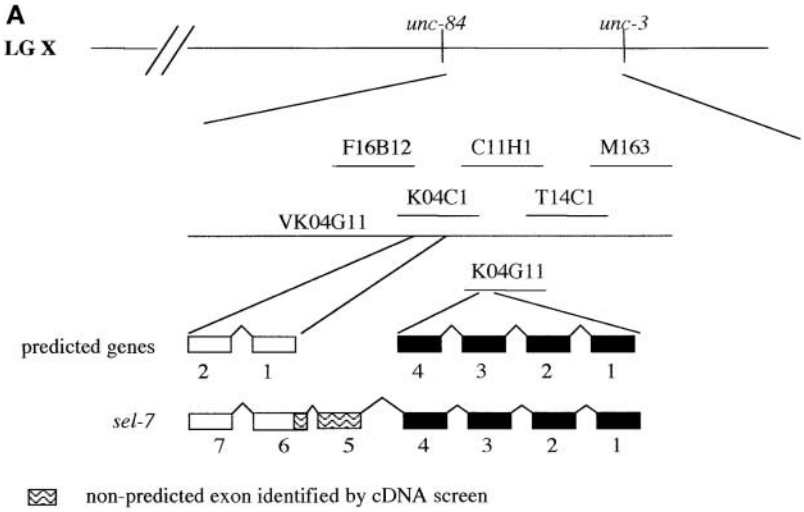

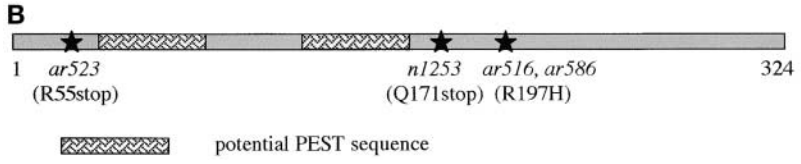

C

```
C. elegans: 1   MAQPNQPTPQFQMAQIPLAAFFDNNESKTMLNSMNLRLNDMDLKLSLILE
C. briggsae:    ------------MAQIPLAAFFDNNESKTILNSMSHRLNDMDLKLSLILE
A. ceylanicum:  ------------MAQLPSIAILDP-DSKTLLNRLNIRLNEIDLKLSIVLE
O. volvulus:    --------------------------------------------------
B. malayi:      --------------------------------------------------

C. elegans: 51  LLATRLPDQRLPSIFTSPPQTVISEAPPQSFTPSATNSTSDKTSSSLK----
C. briggsae:    LLATRLPDQRIPSIFTSPPQTVISEAPPQSFTPSATNSTSDKTTSSLKSLFQ
A. ceylanicum:  LLATRLPDQRLTSILASPPQTLISEASPQSFTPLAGNSASDKTASPKM----
O. volvulus:    --------------------------------------------------
B. malayi:      --------------------------------------------------

C. elegans: 99  TELKTEDSDGDLDMEGEEDTEELFDNESQPSQRNQSPK-ETEVEDEKVLADGP
C. briggsae:    AEIKTEDSDGDLDMEGEEDTEELFENESQPSQRNQSPK-ETEVEDEKVLADGP
A. ceylanicum:  ECKD--DSDGDLDMEGDNENDAEEDFCEQDQTPNAGSR-EQDVK--ATFSDGP
O. volvulus:    ------------DSEGDEEEVDDYDDELDEDVATTNQDRETKI----IHAESN
B. malayi:      --------------------------------------------------

C. elegans: 151 FPEGAVKRAAEKAARSFQSTQPKVFAWQILRESVTDDELRNVQISLRTFH
C. briggsae:    FPEGAVKRAAEKAARSFQSTQPKVFAWQILRESVTDDELRNVQISLRTFH
A. ceylanicum:  FPEGAVKRAAEKAARSFQSTQPKVFAWQILRESVTDEELRNVQISLRTFH
O. volvulus:    FPXGAVRRAAEKAARSFQSTQPKVFAWQILRESVTDQELRNVHISLRTFH
B. malayi:      ----------------------------------KLRNVHISLRTFH

C. elegans: 201 GETADHLLGRQLPKIRLVVEATMKYFKWDLLSTESQLSKAKLILSHLKNN
C. briggsae:    GETADHLLARQLPKIRLVVEATMRYFKWESLSTEGQLGKAKLILSHLKNN
A. ceylanicum:  GE ------------------------------------------------
O. volvulus:    GETAEHLLSRQLPKIRLVVEATMSYFKWDQLSDENQLTKAKLFLSH----
B. malayi:      GETADHLLSRQLPKIRLVVEATMSYFKWDQLSDENQLTKAKLLLSHLKNN

C. elegans: 251 AKVRNWTLREGRPNRVAPATPPVNVDLVWKRYLALLGPAGFT--GILPNLPQ
C. briggsae:    AKVRNWTLREGRPNRVAPATPPVNVDMVWKRYLALLSPANFAT-GILPNLAQ
A. ceylanicum:  --------------------------------------------------
O. volvulus:    --------------------------------------------------
B. malayi:      AKVRNWTLREGRPNRISN-----TMDAVWKRYAAFLGQTSLATVGLLPS---

C. elegans: 301 NLCNGGTQSPSIPQIDPSLFKVDA
C. briggsae:    NLCNGGTQSPTIPQIDPSIFKVES
A. ceylanicum:  ------------------------
O. volvulus:    ------------------------
B. malayi:      ------------------------
```

FIGURE 1.—Molecular cloning and DNA sequence analysis of *sel-7*. (A) Mapping and cloning of *sel-7*. Only the relevant genes and cosmids are shown. (B) Schematic of the SEL-7 protein. The SEL-7 cDNA sequence is in GenBank (accession no. AY 398504). (C) Protein alignment of *C. elegans* SEL-7 and its apparent orthologs in *C. briggsae* (CBP15881), in *A. ceylanicum* (CB175283), in *O. volvulus* (AW208316), and in *B. malayi* (AA071502). Each of the SEL-7 homologs was aligned with SEL-7 sequence using program ClustalW, and the alignments are superimposed here.

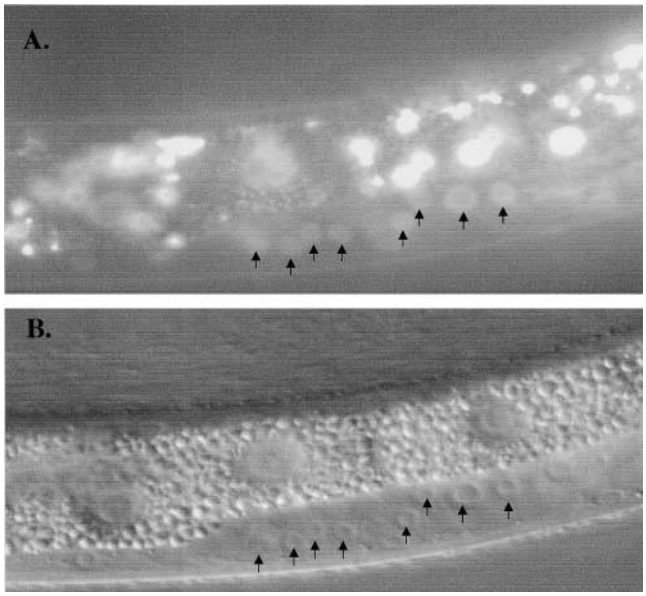

FIGURE 2.—SEL-7 is restricted to the nuclei. Shown here is an L3 larva with arrows pointing to the GFP expression in the gonad. The worm is shown under (A) GFP filter and (B) Nomarski optics.

The carboxy-terminal-tagged SEL-7::GFP fusion protein expressed from *arEx434*, under the control of *sel-12* regulatory sequences, can be visualized in living worms. It is nuclear in the developing gonad (Figure 2) and elsewhere (data not shown). The sequence analysis and subcellular localization of SEL-7 taken together indicate that SEL-7 is a novel nuclear protein.

SEL-7::GFP fusion protein, tagged at the amino-terminus, expressed from *sel-7* genomic sequences, is also nuclear (data not shown). Unfortunately, transgenes containing these constructs are poorly expressed and become silenced, so we were not able to assess the function of these proteins or determine a meaningful *sel-7* expression profile using them. However, we note that these transgenes did display nuclear GFP in the VPCs; perhaps there is a function of SEL-7 in the VPCs that is not detectable as suppression of the Multivulva phenotype of *lin-12(n950)* by loss of *sel-7* activity.

TABLE 4

SEL-7 self-associates but does not interact with components of the LAG-1 nuclear complex

	pAD					
pBD	Empty	LAG-1[b]	LIN-12[c]	SEL-7	SKIP	SEL-8
Empty	—	—	—	—	—	—
LAG-1[a]	—	—	+	—	—	—
LIN-12[d]	—	++	—	—	—	—
SEL-7	—	—	—	++	—	—

Filters were incubated at 37°. ++, the yeast patch turned blue within 1 hr of incubation; +, the yeast patch turned blue after 4 hr; —, no blue after overnight incubation. For plasmid details, see MATERIALS AND METHODS.

[a] Truncated LAG-1 starting at Met203 is used for pBD fusion.

[b] Full-length LAG-1 is inserted into pAD.

[c] Full intracellular domain of LIN-12 spanning from Pro930 to the end of the protein is inserted into pAD.

[d] Part of LIN-12 intracellular domain starting from Pro930 and ending at Val1320 is inserted into pBD.

Analysis of SEL-7 protein-protein interactions with components of the LIN-12(intra) nuclear complex: The apparent nuclear localization of SEL-7 and its function as a positive regulator of *lin-12* activity suggested the possibility that SEL-7 is a component of the nuclear complex that transduces LIN-12/Notch activity. We therefore used the yeast two-hybrid system to explore whether SEL-7 displays physical associations with the following known components of the nuclear complex: LIN-12(intra), LAG-1, SEL-8, and SKIP. Constructs that encode SEL-7 fused to the GAL4 DNA-binding domain or to the GAL4 activation domain were cotransformed into yeast with constructs expressing hybrid proteins containing one of the LIN-12 pathway nuclear components named above or SEL-7 itself. We found that SEL-7

TABLE 5

Three-hybrid assays do not link SEL-7 to the LAG-1 nuclear complex

	pBD-LIN-12[a]		pBD-LAG-1[b]		pBD-SEL-7		
pAD	pRST	pRST-LAG-1[c]	pRST	pRST-LIN-12[d]	PRST	pRST-LAG-1[c]	pRST-LIN-12[d]
SEL-8	—	++	—	++	—	—	—
SEL-7	—	—	—	—	—	—	—
SKIP	/	/	/	/	—	—	—

Filters were incubated at 37°. ++, the yeast patch turned blue within 1 hr of incubation; +, the yeast patch turned blue after 4 hr; —, no blue after overnight incubation; /, not tested. For plasmid details, see MATERIALS AND METHODS.

[a] Part of LIN-12 intracellular domain starting from Pro930 and ending at Val1320 is inserted into pBD.

[b] Truncated LAG-1 starting at Met203 is used for pBD fusion.

[c] Full-length LAG-1 is inserted into pRST.

[d] Full intracellular domain of LIN-12 spanning from Pro930 to the end of the protein is inserted into pRST.

TABLE 6

Assessment of potential SEL-7 interactors using RNAi

dsRNA	*lin-12(n302)*	*lin-12(ar170); unc-3*[a]	*sel-4(n1259)*[a]	*sel-7(n1253) unc-3*[a]
Empty vector	0 (42)	38% (55)	95% (39)	96% (25)
F13B10.1B	0 (64)	47% (99)	96% (49)	97% (33)
K08E3.8	0 (65)	22% (79)	97% (35)	96% (53)
SEL-7	13% (60)	22% (72)	80% (34)	100% (39)

RNAi was performed by feeding. Experiments were done at 20° and scored in parallel. The percentage of hermaphrodites with 1AC (*n*) is shown.

[a] Also contains *arIs51[cdh3::gfp]* as an AC marker.

appears to self-associate, but does not display any interaction with other components of the LIN-12 nuclear complex (Table 4).

As SEL-8 can be detected in a complex with LAG-1 and LIN-12(intra) only when both are present (Petcherski and Kimble 2000a), using a three-hybrid assay we assessed whether this was also the case for SEL-7 (materials and methods). SEL-7 did not show any interaction even when both LAG-1 and LIN-12(intra) were provided (Table 5). We also tested interaction of SEL-7 and SKIP (Zhou *et al.* 2000), providing either LAG-1 or LIN-12(intra) in the hybrid vector. Again, we did not observe any interaction. Thus, if SEL-7 is a component of the nuclear complex, it may not interact directly with any of these known components.

Identification of potential SEL-7-binding proteins using yeast two-hybrid screening: We performed a yeast two-hybrid screen for proteins that interact with SEL-7, hoping to find an interaction partner that would illuminate SEL-7 function. After screening 7.5×10^5 transformants, we identified seven positive clones that satisfied our screening criteria (see materials and methods). One clone corresponded to the predicted gene F13B10.1b, which encodes a protein with two sterile α-motif domains; the other six clones corresponded to the predicted gene K08E3.8, which encodes a protein with a prion (asparagine- or glutamine-rich) domain.

We evaluated the function of these two putative interacting proteins using RNAi. First, we fed wild-type hermaphrodites with bacteria expressing dsRNA for each of the two genes, but observed no obvious phenotypes (data not shown). Then, we performed RNAi assays in sensitized backgrounds and looked for effects on the AC/VU decision comparable to those caused by loss of *sel-7* activity (Table 6). Neither F13B10.1B nor K08E3.8 suppresses the 0 AC-Egl phenotype of *lin-12(n302)* or displays a synergistic effect with *sel-4*. (*sel-4*, an as-yet-uncloned *sel* gene, displays a synthetic 2AC phenotype

TABLE 7

Reassessment of the enhancement of the 2AC phenotype of *lin-12(ar170)* by RNAi

Assay	Empty vector	F13B10.1B	K08E3.8	*sel-7*
1	48% (21)	38% (29)	19% (21)	0 (13)
2	38% (29)	32% (25)	15% (27)	9% (22)
3	37% (30)	45% (33)	13% (23)	6% (16)
4	49% (35)	59% (34)	37% (30)	19% (27)
5	47% (30)	43% (35)	20% (30)	12% (25)
6	48% (50)	50% (20)	37% (27)	9% (34)
Total[a]	45% (195)	45% (176)	24% (158)	10% (137)
Significance[b]	NA	0.0522 (no)	*4.0183 (yes)*	*6.7072 (yes)*

Multiple assays and statistical calculations were used to assess whether there is really an effect on *lin-12(ar170)*. Italics indicate a significant difference from negative control. The percentage of hermaphrodites with 1AC (*n*) is shown. The strain *lin-12(ar170)* contains *unc-3(e151)* and *arIs51[cdh3::gfp]* as an AC marker.

[a] The total percentage is calculated by adding up all the 1AC animals and dividing this number by the total number of animals scored (total *n*).

[b] The following equation was used to assess the significance between F13B10.1B, K08E3.8, *sel-7*, and the negative control, the empty vector: $(p_2 - p_1)/\sqrt{p(1-p)(1/n_1 + 1/n_2)} \rightarrow Z \sim N(0, 1)$, where $p = (X_1 + X_2)/(n_1 + n_2)$, $X_1 \sim \text{Bin}(n_1, p_1)$, $X_2 \sim \text{Bin}(n_2, p_2)$, where n is the total number of worms examined in each RNAi category, X is the total number of worms that had 1AC, and $p = X/n$. When the total number (n) is large, this binomial distribution approaches normal distribution; thus when the value calculated using the above equation is >1.96, the significance level is >95%. The difference between F13B10.1B and the negative control is not significant, whereas the difference between K08E3.8 or *sel-7* and the negative control is significant.

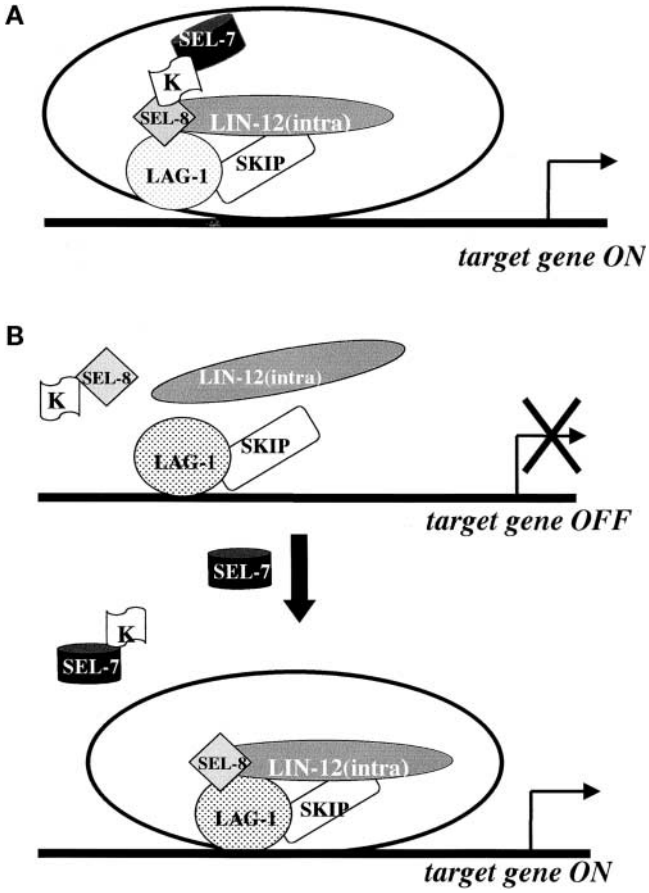

FIGURE 3.—Models for SEL-7 function. (K, K08E3.8). (A) Component of nuclear complex. (B) Facilitated assembly of nuclear complex.

in combination with *sel-7*; J. CHEN, I. KATIC and I. GREENWALD, unpublished observations). However, K08E3.8 weakly enhanced the 2AC phenotype of *lin-12(ar170)* to a degree comparable to *sel-7* RNAi, suggesting that K08E3.8 may function along with SEL-7 (Table 7).

We also used the yeast two-hybrid system to test whether F13B10.1B and K08E3.8 might interact with LIN-12(intra), LAG-1, SEL-8, and SKIP, the known nuclear complex components. Both F13B10.1B and K08E3.8, like SEL-7, self-associate. The only other interaction observed was between K08E3.8 and SEL-8. Like SEL-8, K08E3.8 is also glutamine rich, so we wondered if, like SEL-8, K08E3.8 would interact with LAG-1 or LIN-12(intra). However, K08E3.8 did not show any interaction when both LAG-1 and LIN-12(intra) were present in a three-hybrid assay.

Given that K08E3.8 interacts with both SEL-7 and SEL-8, but SEL-7 and SEL-8 do not interact, we wondered whether K08E3.8 can serve as a bridge between the two proteins. We therefore performed a three-hybrid assay using these three proteins with SEL-7 fused to the GAL4-DB domain, SEL-8 to GAL4-AD domain, and K08E3.8 in pRST, but did not observe any interaction (data not shown).

DISCUSSION

We have shown that alleles that reduce or eliminate *sel-7* activity lead to a reduction in the level of *lin-12* activity. These observations suggest that *sel-7* is a positive regulator of *lin-12* activity. Loss of *sel-7* activity can suppress the effects of two different constitutively activated forms of LIN-12, caused by either missense mutations affecting the extracellular domain or expression of the LIN-12 intracellular domain, which mimics the proteolytic cleavage product. This observation is consistent with, but does not prove, *sel-7* action downstream of activated LIN-12.

sel-7 encodes a novel nuclear protein. By sequence analysis, there appear to be orthologs in other nematodes, but not in more distant phyla. This observation is reminiscent of SEL-8, which also encodes a novel nuclear protein (DOYLE *et al.* 2000; PETCHERSKI and KIMBLE 2000a). However, on the basis of the presence of SEL-8 in a ternary complex with LAG-1 and the intracellular domain of GLP-1, a plausible case can be made that SEL-8 performs a function similar to that of Mastermind in Drosophila and mammals (PETCHERSKI and KIMBLE 2000a; WU *et al.* 2000; KITAGAWA *et al.* 2001). If there is a counterpart to SEL-7 in other organisms, it must be highly diverged in primary sequence.

In the case of *sel-8*, an integral role in LIN-12/Notch signaling was evident from phenotypic analysis (DOYLE *et al.* 2000). In the case of *sel-7*, the case is less clear. The effect of *sel-7* on *lin-12* activity is seen only for a subset of *lin-12-* or *glp-1*-mediated cell fate decisions in sensitized genetic backgrounds; a *sel-7* null allele does not display any overt phenotypic defects (TAX *et al.* 1997 and this study). We do not know whether the restricted effect of *sel-7* in sensitized backgrounds and the lack of a visible phenotype in the absence of *sel-7* activity reflect functional redundancy with another component or complex or a more limited role for *sel-7* as an effector of *lin-12* activity. Although there is no predicted protein in the *C. elegans* genome that seems highly similar to *sel-7*, it may be that functional redundancy is afforded by a protein that is not related in primary sequence.

We speculate that SEL-7 might have a role in the assembly or function of the nuclear complex that includes LAG-1, LIN-12(intra), and SEL-8 (Figure 3). Although we have not detected a direct physical interaction with known components of the nuclear complex, we did identify one protein, K08E3.8, which can interact physically with SEL-7 and SEL-8, and which genetically appears able to influence *lin-12* activity in a sensitized background. Although it would be premature to infer a role for SEL-7 or K08E3.8 on this basis, we note that, although our own analyses did not identify clear rela-

tives of K08E3.8 (data not shown), Wormbase Release WS109 (http://www.wormbase.org) lists related human and yeast proteins that have functions in transcriptional regulation. At least five additional *sel* genes are defined by conventional genetic screens (Tax *et al.* 1997; L. Vallier, I. Katic, J. Chen and I. Greenwald, unpublished observations) and many more identified by RNAi screens (C. Bais and I. Greenwald, unpublished observations). Among these as-yet-uncharacterized *sel* genes there may be components that link SEL-7 to the nuclear complex or to other aspects of *lin-12/Notch* signaling.

We thank Iskra Katic and Natalie De Souza for helpful comments on the manuscript. This work was supported by National Institutes of Health grant CA-095389 (to I.G.). I.G. is an Investigator of the Howard Hughes Medical Institute.

LITERATURE CITED

Ailion, M., and J. H. Thomas, 2000 Dauer formation induced by high temperatures in *Caenorhabditis elegans*. Genetics **156:** 1047–1067.

Brenner, S., 1974 The genetics of *Caenorhabditis elegans*. Genetics **77:** 71–94.

De Strooper, B., W. Annaert, P. Cupers, P. Saftig, K. Craessaerts *et al.*, 1999 A presenilin-1-dependent gamma-secretase-like protease mediates release of Notch intracellular domain. Nature **398:** 518–522.

Doyle, T. G., C. Wen and I. Greenwald, 2000 SEL-8, a nuclear protein required for LIN-12 and GLP-1 signaling in *Caenorhabditis elegans*. Proc. Natl. Acad. Sci. USA **97:** 7877–7881.

Fares, H., and I. Greenwald, 1999 SEL-5, a serine/threonine kinase that facilitates *lin-12* activity in *Caenorhabditis elegans*. Genetics **153:** 1641–1654.

Fares, H., and I. Greenwald, 2001 Genetic analysis of endocytosis in *Caenorhabditis elegans*: coelomocyte uptake defective mutants. Genetics **159:** 133–145.

Greenwald, I., 1998 LIN-12/Notch signaling: lessons from worms and flies. Genes Dev. **12:** 1751–1762.

Greenwald, I., and G. Seydoux, 1990 Analysis of gain-of-function mutations of the *lin-12* gene of *Caenorhabditis elegans*. Nature **346:** 197–199.

Greenwald, I., P. W. Sternberg and H. R. Horvitz, 1983 The *lin-12* locus specifies cell fates in *Caenorhabditis elegans*. Cell **34:** 435–444.

Hodgkin, J., A. Papp, R. Pulak, V. Ambros and P. Anderson, 1989 A new kind of informational suppression in the nematode *Caenorhabditis elegans*. Genetics **123:** 301–313.

Hubbard, E. J., Q. Dong and I. Greenwald, 1996 Evidence for physical and functional association between EMB-5 and LIN-12 in *Caenorhabditis elegans*. Science **273:** 112–115.

Karp, X., and I. Greenwald, 2003 Post-transcriptional regulation of the E/Daughterless ortholog HLH-2, negative feedback, and birth order bias during the AC/VU decision in *C. elegans*. Genes Dev. **17:** 3100–3111.

Kitagawa, M., T. Oyama, T. Kawashima, B. Yedvobnick, A. Kumar *et al.*, 2001 A human protein with sequence similarity to *Drosophila* Mastermind coordinates the nuclear form of Notch and a CSL protein to build a transcriptional activator complex on target promoters. Mol. Cell. Biol. **21:** 4337–4346.

Levitan, D., and I. Greenwald, 1995 Facilitation of *lin-12*-mediated signalling by *sel-12*, a *Caenorhabditis elegans* S182 Alzheimer's disease gene. Nature **377:** 351–354.

Levitan, D., and I. Greenwald, 1998 Effects of SEL-12 presenilin on LIN-12 localization and function in *Caenorhabditis elegans*. Development **125:** 3599–3606.

Mello, C., and A. Fire, 1995 DNA transformation. Methods Cell Biol. **48:** 451–482.

Pepper, A. S., D. J. Killian and E. J. Hubbard, 2003 Genetic analysis of *Caenorhabditis elegans glp-1* mutants suggests receptor interaction or competition. Genetics **163:** 115–132.

Petcherski, A. G., and J. Kimble, 2000a LAG-3 is a putative transcriptional activator in the *C. elegans* Notch pathway. Nature **405:** 364–368.

Petcherski, A. G., and J. Kimble, 2000b Mastermind is a putative activator for Notch. Curr. Biol. **10:** R471–R473.

Pettitt, J., W. B. Wood and R. H. Plasterk, 1996 *cdh-3*, a gene encoding a member of the cadherin superfamily, functions in epithelial cell morphogenesis in *Caenorhabditis elegans*. Development **122:** 4149–4157.

Priess, J. R., H. Schnabel and R. Schnabel, 1987 The *glp-1* locus and cellular interactions in early *C. elegans* embryos. Cell **51:** 601–611.

Struhl, G., and I. Greenwald, 1999 Presenilin is required for activity and nuclear access of Notch in *Drosophila*. Nature **398:** 522–525.

Struhl, G., K. Fitzgerald and I. Greenwald, 1993 Intrinsic activity of the Lin-12 and Notch intracellular domains *in vivo*. Cell **74:** 331–345.

Tax, F. E., J. H. Thomas, E. L. Ferguson and H. R. Horvitz, 1997 Identification and characterization of genes that interact with *lin-12* in *Caenorhabditis elegans*. Genetics **147:** 1675–1695.

Timmons, L., and A. Fire, 1998 Specific interference by ingested dsRNA. Nature **395:** 854.

Timmons, L., D. L. Court and A. Fire, 2001 Ingestion of bacterially expressed dsRNAs can produce specific and potent genetic interference in *Caenorhabditis elegans*. Gene **263:** 103–112.

Weinmaster, G., 2000 Notch signal transduction: a real rip and more. Curr. Opin. Genet. Dev. **10:** 363–369.

Wen, C., M. M. Metzstein and I. Greenwald, 1997 SUP-17, a *Caenorhabditis elegans* ADAM protein related to Drosophila KUZBANIAN, and its role in LIN-12/NOTCH signalling. Development **124:** 4759–4767.

Wu, L., J. C. Aster, S. C. Blacklow, R. Lake, S. Artavanis-Tsakonas *et al.*, 2000 MAML1, a human homologue of *Drosophila* Mastermind, is a transcriptional co-activator for NOTCH receptors. Nat. Genet. **26:** 484–489.

Zhou, S., M. Fujimuro, J. J. Hsieh, L. Chen and S. D. Hayward, 2000 A role for SKIP in EBNA2 activation of CBF1-repressed promoters. J. Virol. **74:** 1939–1947.

Communicating editor: B. J. Meyer